Presented at the 2011 SME Annual Meeting & Exhibit
Feb. 27-Mar. 2, Denver, CO

Mechanisms for Flotation of Fine Oil Droplets

C. Hank Rawlins, PhD, P.E., eProcess Technologies

ABSTRACT

The oil and gas industry produces 5-7 barrels (0.795-1.113 m³) of water for each barrel (0.159 m³) of oil. This produced water must be separated from and cleaned of hydrocarbon fluids before disposal or reinjection. Hydraulic or mechanical flotation cells are a common method of removing fine (<100 μm) oil droplets from produced water, however this application has undergone far less investigation compared to traditional mineral flotation. Produced water is hypersaline (up to 300,000 ppm dissolved solids) and the flotation gas is methane, both of which affect the interfacial tension relationship between the three-phase droplet-water-bubble system. Oil droplets in this size range are nearly perfect spheres thus the surface area for attachment approach is smaller compared to an irregular mineral grain. Oil droplets are naturally buoyant and hydrophobic, thus chemical additions are rarely used. Flotation is used to decrease vessel residence time and not provide a concentration function. All of these factors lead to unique features required by an oil droplet flotation cell. The goal of this project is to research the mechanisms by which fine oil droplets are captured and conveyed by gas flotation. The mechanisms being investigated include attachment by free energy minimization, hydrodynamic wake transfer, formation of aggregate buoyant mats, and gas bubble nucleation and growth.

OILFIELD MINERAL PROCESSING

World crude oil production averaged 73.8 million barrels per day (BPD) (11.7 million m³/d) in 2008 (DOE/EIA), however, the total amount of water produced along with the crude oil fluids totaled over 194 million BPD (30.8 million m³/d) (Veil 2009), resulting in approximately 3 barrels (0.477 m³) of water produced along with 1 barrel (0.159 m³) of crude oil. Termed "produced water" this liquid occupies production volume and requires expense for treatment and disposal. The volume of produced water is often the limiting factor for sizing the entire production system. While the U.S. Environmental Protection Agency (EPA) sets oil and grease discharge limits (in produced water) for territorial seas (0-3 miles) and the outer continental shelf (>3 miles) at 29 mg/l monthly average and 42 mg/l daily maximum, the general trend worldwide regarding produced water is towards zero discharge. Reinjection into the production formation or a separate zone is the only viable route to reach zero discharge. To prevent disposal well damage, the produced water contaminants such as suspended silts, clays, scale, oil droplets, and bacteria, must be removed to prevent near well-bore formation plugging, invasive plugging, perforation plugging, or wellbore fill-up (Barkman and Davidson 1972). These solid and liquid contaminants are removed in a series of steps that utilize many traditional mineral processing unit operations specifically designed for oilfield use.

OFFSHORE PRODUCED WATER TREATMENT

Produced water is treated with hydrocyclones, flotation cells, and filtration vessels (Rawlins 2009 SME). The first stage after leaving a production separator is removal of inorganic solid particulates using a closed underflow multi-liner solid-liquid hydrocyclone vessel termed a "desander" (Rawlins and Wang 2002). The produced water stream is then treated with a multi-liner liquid-liquid hydrocyclone vessel termed a "deoiler". Dispersed oil droplets greater than 50-75 microns are captured to form a continuous oil concentrate (<10% oil) reject stream which is sent to the dehydrator or a slop tank for oil recovery. Details of the design and operation of a deoiler system are given elsewhere (Ditria and Hoyack 1994). Produced water exiting the deoiler contains up to 50 ppmv of oil (thus 90-98% removal efficiency by the deoiler) with a median droplet size <50 microns. As a point of reference for this paper the term fine oil droplets applies to a median droplet size <50 microns in a very dilute system (<50 ppmv).

A flotation cell is the primary unit operation used to recover fine oil droplets from produced water systems. Both mechanical induced gas flotation (IGF) and hydraulic dissolved gas flotation (DGF) cells have been used for residual oil removal from produced water since the late 1960's (Sport 1970; Bassett 1971). Mechanical IGF cells were developed from the WEMCO® multi-cell rectangular-shaped mechanically-driven rotor/stator design. The primary difference from a mineral processing flotation cell is that the flotation chamber is fully encapsulated to prevent hydrocarbon vapor release into the atmosphere. Mechanical IGF cells have found significant use in applications that are not space or motion sensitive such as land-based or fixed-platform fields. However deepwater floating platforms are not suitable for mechanical IGF

use as the footprint requirements are too strict and motion of the platform does not allow a fixed skimming level for the oil froth resulting in re-entrainment of the oil or splashing of the produced water. The current generation of offshore flotation cell design is a compact hydraulic IGF with a vertical orientation and no moving parts. Figure 1 shows a vertical IGF cell installed on an offshore fixed-platform. The vertical orientation both minimizes footprint, but also allows a thicker oil skim pad which is much less sensitive to platform motion. Vertical hydraulic IGF cells are similar in concept to a column flotation cell; however the length to diameter ratio is normally 3:1, whereas a column cell may be 10:1. These flotation cells rely partly on dissolved gas effervescing from solution (due to pressure letdown), but the primary bubble source is hydraulic entrainment of gas through an eductor, sparger, or shear pump. In all cases the flotation gas is natural gas sources from the facility. Air is never used as the flotation gas, as oxygen in the system can lead to adverse chemical reactions, corrosion, or biological growth. A flotation cell will generally reduce the oil concentration to <25 ppmv and capture oil droplets down to a median size of <20 microns. Currently eight companies provide over twenty different models of flotation cells specifically designed for produced water filtration (Rawlins 2009).

Figure 1. Vertical IGF cell (gray vertical vessel near center) installed on an offshore fixed-platform.

FLUID PROPERTIES IN PETROLEUM CIRCUITS

In flotation of fine oil droplets in a petroleum production water treating circuit, the continuous phase is produced water. Produced water differs significantly from the fresh/recycled water used in mineral processing circuits in the amount of dissolved solids. All formation (produced) water contains substantial concentrations of dissolved solids, primarily sodium chloride. The concentration and distribution of ions differ greatly from seawater giving produced water unique properties. Total dissolved solids (TDS) concentrations have been reported from 200 ppmw to saturation, which is near 300,000 ppmw (McCain 1990). Typical values lie in the range of 80,000-120,000 ppmw, which is 3-4 times the TDS value of seawater. The most common cations are Na^+, Ca^{2+}, and Mg^{2+}, and the most common anions are Cl^-, SO_4^{2-}, and HCO_3^-.

Produced Water

In modeling the mechanisms of fine oil droplet flotation in produced water, the properties of the continuous fluid are required. The density and viscosity are needed for a simple Stokesian buoyancy calculation, while further calculations on bubble-droplet interaction require the interfacial tensions (water-oil and water-gas). These thermophysical properties are a function of pressure, temperature, and water composition. Of these factors, temperature and composition are determining while the pressure normally exhibited in a flotation cell (<689 kPa) has a negligible effect. Figure 2 shows the effect of temperature and salinity on water density and viscosity at atmospheric pressure.

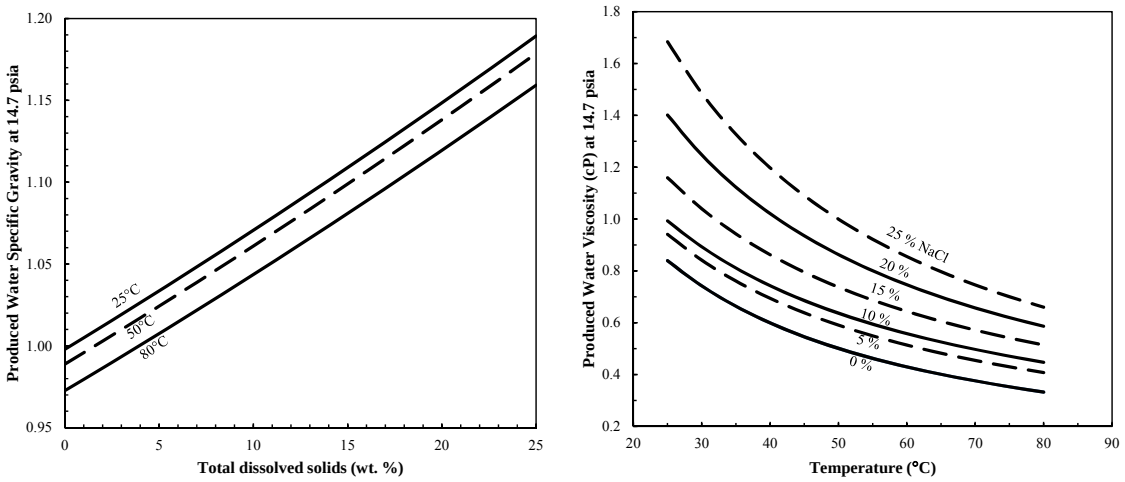

Figure 2. (left) The effect of dissolved solids (as salinity) and temperature on the specific gravity of produced water (data from McCain 1990 and Street et al. 1996) and (right) the effect of salinity and temperature on the viscosity of produced water (data from McCain 1990).

Temperature and salinity have competing effects on both density and viscosity. An increase in temperature decreases both properties, while an increase in dissolved solids has a direct proportional effect. Temperature has a stronger effect on viscosity and dissolved solids content a stronger effect on density. In terms of Stokes' Law, both density and viscosity have unity exponent, however, the density term is a relative factor between oil and water (ρ_{water}-ρ_{oil}) while viscosity is a direct factor. Temperature has a slightly stronger effect on viscosity than salinity. For a given droplet diameter, doubling the temperature (at a fixed salinity) increases the rise velocity by ~50% and doubling the salinity (at a fixed temperature) decreases the rise velocity by ~10%, therefore temperature is the prevailing parameter. While this discussion has primarily focused on the rise of oil droplets in produced water a similar relationship exists with the rise of gas bubbles in produced water. The density difference between water and gas is several orders of magnitude higher than that between water and oil, but the viscosity effect of the water phase is the same. The net effect is that gas bubbles rise at about one order of magnitude higher velocity compared to a similar diameter oil droplet.

The interfacial tension (IFT) between gas-water (γ_{gw}) and oil-water (γ_{ow}) is a key factor in determining droplet/bubble stability. Figure 3 shows the effect of temperature and salinity on gas-water and oil-water IFT at ambient pressure. The left curve showed gas-water IFT, with air-water IFT given as a point of reference, and shows that increasing temperature decreases IFT. Methane has a slightly lower IFT (3-7%) to fresh water compared to air showing that methane bubbles in water are slightly less stable than air bubbles and the driving force for bubble coalescence is enhanced (Jennings and Newman 1971). The effect of dissolved solids is to increase surface tension. The data shown for methane-water IFT at various salinities is estimated from data for air-water IFT with NaCl molality given at ambient pressure and temperature (Argaud 1992). Increasing the salinity to 10 wt.% solids (NaCl) brings the methane-water IFT to near the same values as air-water. Salinity has the effect to stabilize gas (methane) bubbles and work against bubble coalescence. The magnitude of temperature and salinity effect on methane-water IFT is approximately the same, but working in opposite directions.

The right curve in Figure 3 shows the interfacial tension between oil and water. While methane is a single component gas, and is the most prevalent component of flotation gas used in hydraulic IGF cells, crude oil has a widely varying composition. As a reference, data is presented for n-dodecane ($C_{12}H_{26}$) which has the characteristics of a light crude-oil condensate. It has a specific gravity of 0.80 (46 API) and is a neutral (non-polar) oil. The IFT range for n-dodecane and pure water is about 30% less than the IFT for methane and pure water. Oil droplets are less stable and have a stronger driving force for coalescence compared to bubble-bubble coalescence. The effect of temperature is to decrease IFT, while salinity increases IFT. Compared to methane-water, the magnitude of temperature and salinity effect on IFT is very similar.

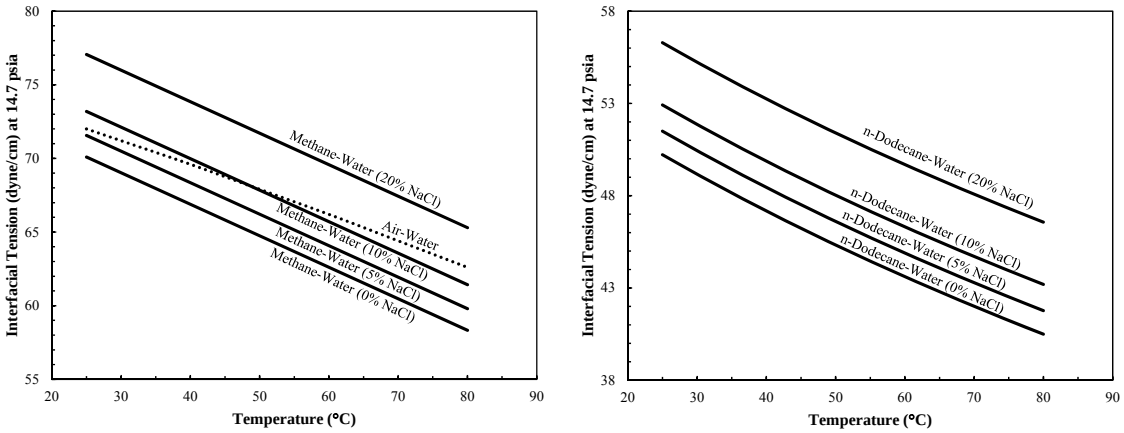

Figure 3. (left) The effect of dissolved solids (as salinity) and temperature on the interfacial tension between methane and water at ambient pressure (data from Jennings and Newman 1971; Street et al. 1996; Argaud 1992) and (right) the effect of salinity and temperature on the interfacial tension between n-dodecane and water at ambient pressure (data from Street et al. 1996; Argaud 1992).

As both methane and n-dodecane are neutral hydrocarbons, the IFT between these compounds is lower than that between either of them and water. Figure 4 shows the IFT between methane gas and n-dodecane liquid across the temperature range 25-80°C (ambient pressure). The IFT value is about 50% less than the IFT between n-dodecane and water. Temperature has a small decreasing effect on IFT over the observed range, reducing the value about 9%. These values disregard the effect of polar hydrocarbons that may be present at the liquid-gas interface, and the effect of dissolved or dispersed solids in the water. All of these factors will increase the IFT between methane and n-dodecane. Decreasing the carbon content of the alkane (C_n) decreases the oil-gas IFT (γ_{og}). Liquid i-Pentane (C_5H_{12}) has approximately half the IFT with methane compared to liquid n-dodecane. Raw crude oil is a mixture of at least 30-40 hydrocarbons (C_1, C_2,…C_n) and the real γ_{og} is often lower than that shown in Figure 4.

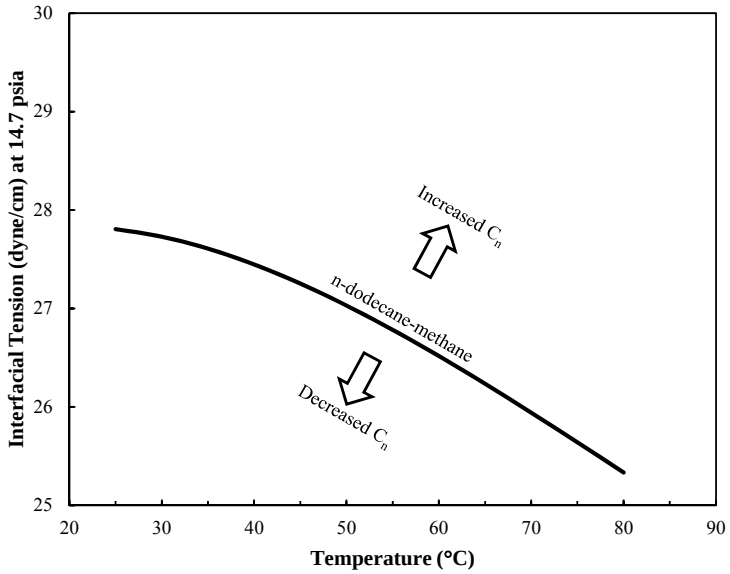

Figure 4. The effect of temperature on the interfacial tension between methane and n-dodecane (data from McCain 1990).

Spreading Coefficient

One method to estimate the efficacy of oil droplet flotation by methane bubbles is to evaluate the spreading coefficient. The spreading coefficient of a fluid (S) is the imbalance between the interfacial tensions acting along the contact line between the fluid phases (Grattoni et al 2003). For the water-oil-gas system, the oil spreading coefficient at the water-gas interface (S_o) is given by Equation 1.

$$S_o = \gamma_{wg} - \gamma_{ow} - \gamma_{og} \quad (1)$$

If ($\gamma_{ow} + \gamma_{og}$) is less than γ_{wg}, then S_o will be positive which indicates spreading of the oil layer to form a boundary between the gas and water. A negative S_o indicates a non-spreading condition, in which the oil will form a finite contact angle with the gas and water interface. Spreading of the oil droplet along the gas-water interface (i.e. formation of an oil coating on the gas bubble) will only happen if the balance of interfacial tensions yields a positive spreading coefficient, therefore gas flotation is more effective with a positive S_o.

Figure 5 shows the effect of temperature and salinity on the spreading coefficient of the dodecane-methane-water system. In pure water a dodecane droplet has a S_o of -7.93 dyne/cm at 25°C. Temperature has a small increasing effect on S_o, raising the value by ~4% when the temperature doubles to 50°C. Salinity has a slightly greater effect increasing S_o by 7% as the salinity doubles from 10% to 20%. In all cases shown S_o is negative indicating that n-dodecane will not spread (or wet) the interface between methane and water, but will form a definite contact angle. Decreasing the carbon content of the alkane (C_n) will increase the spreading coefficient such that light oils (i.e. propane and ethane) or raw crude oils that contain a high content of these light hydrocarbons will actively coat bubbles of methane in a saline-water system. Chemical additions are not commonly used in oil droplet flotation in order to minimize treatment cost, however a surfactant that lowers the oil-water interfacial tension (γ_{ow}) will increase the spreading coefficient to enhance bubble coating by the oil droplet.

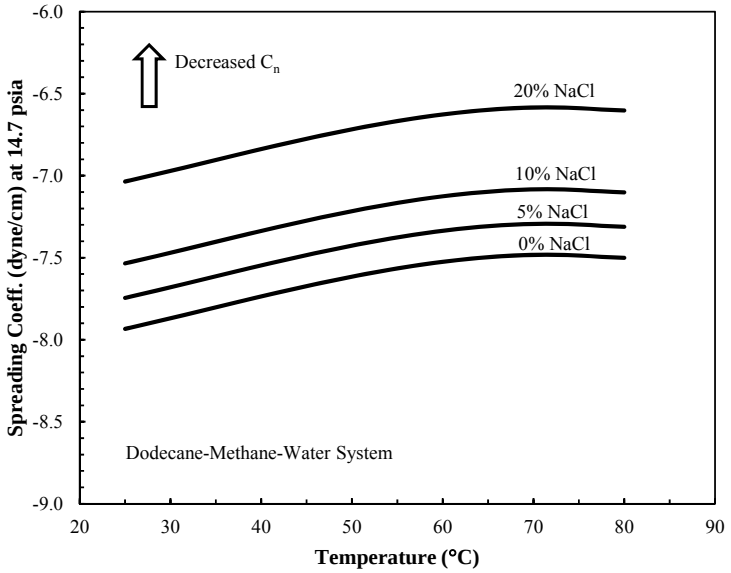

Figure 5. The effect of temperature and salinity on the spreading coefficient of the dodecane-methane-water system.

ATTACHMENT OF OIL DROPLETS TO GAS BUBBLES

Effective flotation relies on attachment of the introduced gas bubble to the dispersed oil droplet. There are numerous factors involved in successful collision and attachment including bubble/droplet size ratio, bubble swarm density, mean bubble size, and bubble distribution, produce water salinity, oil viscosity, spreading coefficient, fluid velocity, and turbulence. Of these factors gas bubble size, distribution, and dispersion are the most important for flotation efficiency. Oil droplets can attach to gas bubbles by four mechanisms, which are depicted graphically in Figure 6.

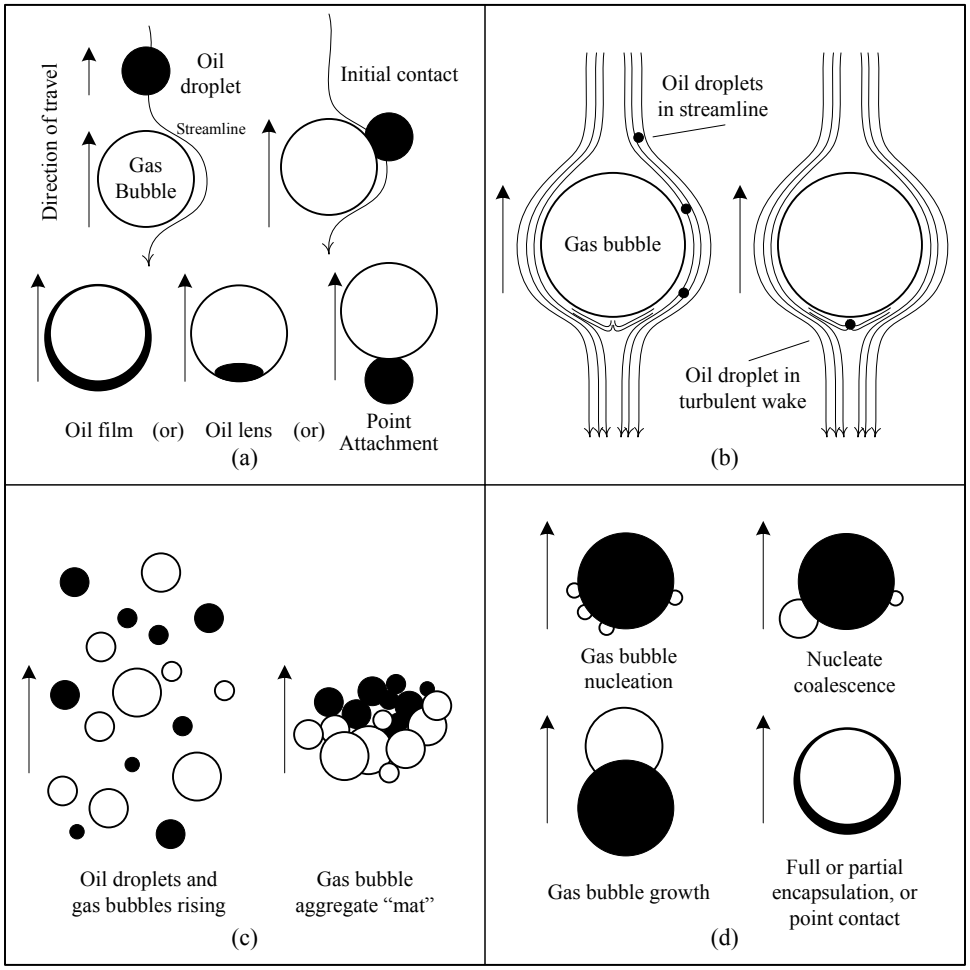

Figure 6. Mechanisms for gas bubble capture of oil droplets suspended in water: (a) direct impingement with full or partial encapsulation by chemical adhesion, (b) hydrodynamic capture of oil droplets in the wake of a rising gas bubble, (c) clustering of gas bubbles to form a buoyant mat, and (d) gas bubble nucleation, coalescence, and growth on the surface of an oil droplet to result in full or partial encapsulation

Mechanisms of Attachment

The primary mechanism for oil droplet flotation is full or partial encapsulation of the gas bubble by the oil droplet as shown in Figure 6a (Strickland 1980; Oliveira et al. 1999; Grattoni et al. 2003; Moosai and Dawe 2003; Niewiadomski et al. 2007). In this mechanism both the oil droplet and gas bubble exhibit buoyant rise in the fluid in the opposite direction of gravity. The velocity of the gas bubble is sufficiently higher than that of the oil droplet due to diameter and density, thus from the gas bubble inertial frame of reference the oil droplet is settling downward as if under gravitational influence. Because the oil droplet has lower inertia than the surrounding water it will not directly impact the gas bubble, and water streamlines formed from the rising bubble tend to direct the approaching droplet around the bubble. As the droplet passes around the bubble the trajectory in the rising wake pulls the droplet towards the bubble, and if the droplet has sufficient diameter the droplet will touch the gas bubble surface. Once the droplet has touched the bubble surface the intervening water film thins then breaks to allow the hydrocarbon liquid and gas to come in contact (Niewiadomski et al. 2007). Attachment of the oil droplet to the gas bubble is governed by the spreading coefficient and free energy minimization. Full encapsulation, where the oil completely covers the gas bubble surface provides the strongest bond between the hydrocarbon liquid and gas thus prevents removal of the oil by shear forces. In addition, an oil coated bubble may more easily attract a free oil droplet thus multiplying the flotation effectiveness (Strickland 1980). Should the droplet size be insufficient for full encapsulation, the oil droplet may form a lens at the aft of the bubble to minimize contact with the

aqueous phase, or if the spreading coefficient is negative the oil droplet may form a point contact with the gas bubble. Lens formation is a stronger bond than point contact.

A second mechanism was shown (Sylvester and Byeseda 1980) when gas bubbles of 200-700 microns diameter were observed to capture oil drops of 1-15 microns diameter in the hydrodynamic wake of the rising bubble, instead of chemical adhesion to the surface. This mechanism is depicted in Figure 6b. The "falling" oil droplet follows the water streamline around the rising bubble. The droplet has insufficient diameter to break the water layer at the bubble surface, however the droplet is small enough to become trapped in the turbulent wake at the aft-end of the rising bubble thus follow the bubble in its upward trajectory. This mechanism does not create a strong bond between the hydrocarbon gas and liquid. However this does provide a mechanism by which large bubbles can capture droplets smaller than the D_{cr}.

A third mechanism postulated is shown in Figure 6c, whereby bubble clusters form a buoyant "mat" to assist in droplet entrapment along with hydrophobic binding (Rodrigues and Rubio 2007). The formation of bubble clusters has been observed in mineral flotation, in which case the bubbles are held together by bridging particles that are simultaneously attached to two or more particles (Fuerstenau et al 2007). In oil flotation, the oil droplets, especially in the case of point attachment, or suspended solids, can act as a bridging structure to form a cluster or mat of bubbles. The bubble mat sweeps upward with a wider diameter than single particles and is able to more effectively sweep the water phase. Bubble coalescence is retarded by high ionic content of the water, plus stabilizing chemicals in the water, thus the bubbles attach to particles (liquid or solid), but do not form a larger bubble. Bubble cluster formation is promoted by high density of small diameter bubbles and a high density of finely disseminated hydrophobic particles.

The fourth mechanism, shown in Figure 6d, is a product of the dissolved gas flotation (DGF) mechanism in that gas bubbles nucleate on particle/droplet surfaces, then grow to sufficient size to aid in flotation as the gas comes out of solution (Oliveira et al. 1999; Rodrigues and Rubio 2007). For this mechanism to take place, sufficient gas must effervesce from solution, which usually coincides with a fairly large pressure drop at the inlet of the flotation cell. Unlike a DGF cell, a separate mechanism for dissolving gas is not utilized, but the gas is forced into solution while the fluids are in contact in the reservoir. Gas will flash from solution at all stages of pressure let-down including well-bore inflow, pipe transport, choke let-down, and inside three-phase separators. The solubility of methane, and other hydrocarbon gases, in water is several orders of magnitude lower than the solubility in hydrocarbon liquid therefore most of the gas effervescing from solution will come from the oil droplets. The gas bubbles will nucleate within the droplets or at the droplet surface, and continue to grow in diameter as long as the partial pressure is lower in the gas phase compared to the liquid phase. Eventually the nucleating bubbles will contact, and may coalesce to form a larger discrete bubble. The coalesced bubble will form full or partial encapsulation or point contact depending on the volume of the bubble and the spreading coefficient, which is similar to the mechanism in Figure 6a. The amount of gas effervescing depends primarily on the pressure and temperature difference between the upstream piping and the operating conditions of the flotation cell, and the composition of the hydrocarbon fluid. These factors determine the bubble-point pressure.

Free Energy Minimization

Analysis of how an oil droplet will interact with a gas bubble upon contact (Figure 6a) can be undertaken by evaluation of the overall change in system energy. The free energy (G) of the interface between a gas bubble and water or an oil droplet and water can be determined from the interfacial tension (γ) and bubble/droplet surface area (A), as shown in Equation 2.

$$\gamma = \left(\frac{\partial G}{\partial A}\right)_{P,T,n} \tag{2}$$

For constant pressure, temperature, and composition then G is a product of γ and A. If the system energy is reduced ($\Delta G<0$) by converting a discrete oil drop and a discrete gas bubble into an aggregate, then the oil will coat or attach to the gas bubble. The creation of an aggregate from the discrete particles can be represented by Equation 3.

$$\left(\gamma_{og} A_{bubble} + \gamma_{ow} A_{oilfilm}\right) - \left(\gamma_{ow} A_{drop} + \gamma_{wg} A_{bubble}\right) < 0 \tag{3}$$

If the energy of the discrete oil droplet ($\gamma_{ow}A_{drop}$) plus the discrete gas bubble ($\gamma_{wg}A_{bubble}$) is greater than the energy of the aggregate then the droplet will attach to or coat the bubble. The oil acts to replace the water-gas interface with an oil-gas interface plus oil-water interface with a net reduction in free energy. The reduction in energy is driven by interfacial tension and droplet:bubble size ratio. As the surface area of the bubble is in both terms, changing the bubble size alone has less effect than changing the droplet:bubble ratio.

A model is under development to study the free energy minimization of the droplet-bubble interaction. The model uses a geometric basis of sphere-sphere intersection of which multiple configurations were studied. These configurations are shown in Figure 7.

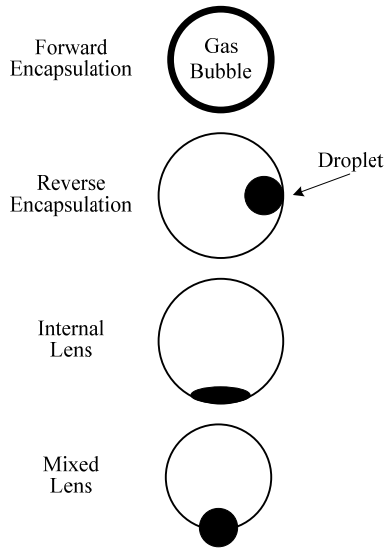

Figure 7. Configurations of droplet-bubble interaction studied for free energy minimization.

Forward encapsulation is complete coating of the bubble by an oil film upon contact, while reverse encapsulation is when the droplet is completely contained within the gas bubble and has only point contact with the water phase. In the latter case, the gas bubble diameter will increase due to the volume of the droplet contained therein. An internal lens also has the volume of the droplet contained, however the oil maintains an interface with both the bubble and water. A mixed lens has the droplet partially contained within the bubble, but maintains a substantial interface with the water. In the case of forward encapsulation the oil coating completely eliminates the bubble-water interface, and with reverse encapsulation the droplet-water interface is eliminated. Both cases involving lens shapes still have all three interfaces. The free energy model only assumes minimization based on interface area, and does not use change in bubble pressure with increased diameter.

Figure 8 shows the net free energy change of the four scenarios identified in Figure 7 based on droplet:bubble diameter ratio. The case shown is for fresh water (0% salinity), ambient temperature, and the methane-dodecane-water system. The lowest free energy configuration changes with droplet:bubble ratio. Full encapsulation takes place at a ratio of 0.74 and higher. The mixed lens does exhibit a small range of optimization from 0.72-0.74, and below 0.72 the primary configuration is an internal lens. Reverse encapsulation is not a dominant mechanism at any ratio, because it does not eliminate any methane-water interface, which has the highest energy. Starting with an equal bubble and droplet diameter, as they intersect the droplet will completely engulf the bubble. As the droplet diameter decreases, the encapsulation layer gets thinner to the point where maintaining closer to the original droplet shape is more energy effective and the droplet starts to pierce the bubble. At a ratio of 0.72 and smaller the droplet is engulfed by the bubble, but the droplet maintains some interface with the water (to minimize the bubble-water interface).

Increasing the salinity to 10%, at 25° C, will increase the methane-water and dodecane-water IFT. The net effect is to expand the region for forward encapsulation down to 0.72. The mixed lens configuration is thus eliminated and an internal lens is the lowest energy shape below 0.72. Increasing the temperature to 75°C, at 0% salinity, decreases the IFT between all three phases. The net effect is to expand mixed lens configuration to cover the range from 0.67-0.77. Above this range

forward encapsulation will take place, and below this range an internal lens will be formed. Thus salinity and temperature have competing effects on the formation of a mixed lens. At 10% salinity and 75°C temperature, the mixed lens formation takes place at 0.71-0.73 droplet:bubble ratio, which is nearly the same region as ambient fresh water.

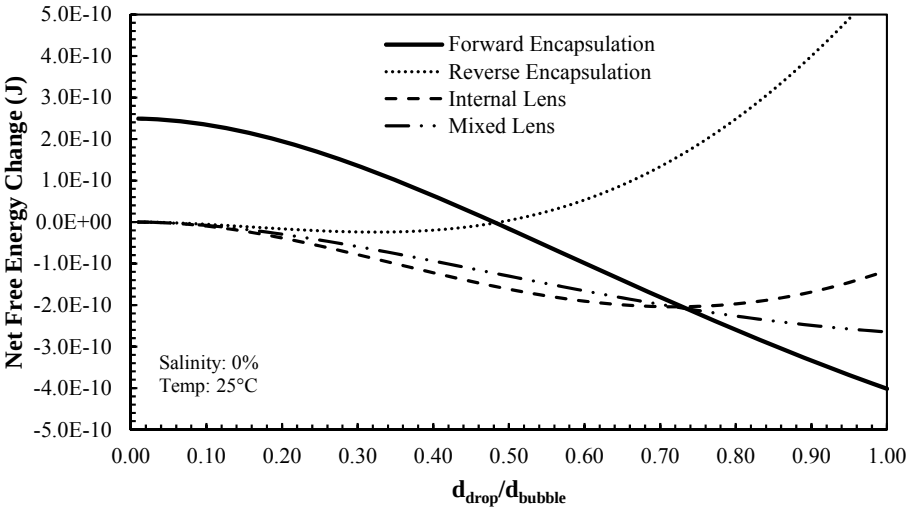

Figure 7. Configurations of droplet-bubble interaction studied for free energy minimization.

Oil droplet capture will take place by a combination of mechanisms. At approximately ¾ droplet:bubble ratio the droplet will engulf the bubble to be captured by full encapsulation. The aggregate has a spherical shape with a hollow core. Below this ratio the bubble will engulf the droplet. The aggregate again has a spherical shape, however the droplet will form a lens at the inside bottom of the bubble. Increasing salinity favors full encapsulation while increasing temperature favors lens formation. These factors are normally not adjustable within a production system however changes to the IFT, bubble diameter, or droplet diameter can be undertaken to improve oil droplet capture. For full encapsulation, decreasing methane bubble size or increasing oil droplet size is important to improve flotation efficiency. Another important factor is to maximize the methane-water interfacial tension. The magnitude of γ_{wg} is larger than γ_{og} or γ_{ow}. Impurities in methane such as higher hydrocarbons, oxygen, or carbon dioxide will all decrease γ_{wg} thus the methane used should be kept clean and pure.

SUMMARY

Treatment of oil well fluids requires the same approach methodology as traditional mineral processing, and uses much of the same unit processes. Approaching the treatment of crude oil as oilfield mineral processing allows technology transfer with the goal of finding optimum solutions for both industries based on two viewpoints. An example is water treatment in the petroleum which requires the removal of small (<100 μm diameter) oil droplets, for which induced gas flotation is commonly employed. Oil flotation differs from mineral flotation in that oil droplets are naturally hydrophobic, have a lower density than water, and have a spherical shape. Unlike mineral particles, oil droplets have a very low energy of cohesion (35-56 dyne/cm for oil vs. 2000-5000 dyne/cm for minerals) and are subject to breakup from water shear forces, or may coalesce upon contact with other oil droplets (Gutkowski et al. 1981). Produced water has increased density, viscosity, and IFT with hydrocarbon fluids due to the high content of dissolved solids (mainly NaCl). The IFT between the three phases drives the spreading coefficient and critical bubble:droplet diameter ratio to determine how oil and gas bubbles will interact. Once an oil droplet contacts a methane gas bubble it will attach through one of four mechanisms, of which complete encapsulation provides the strongest bond. Complete encapsulation occurs when the droplet diameter is at least 0.7 times the diameter of the gas bubble. The droplet-bubble aggregate then rises faster than the oil droplet alone, which provides the impetus for using gas flotation. The rise velocity of oil droplets or gas bubbles is governed by Stokes relationship, and because of the several of orders of magnitude increase in rise velocity, the residence time and size of the flotation cell can be significantly reduced compared to gravity separation. Offshore produced water treatment uses primarily a vertical hydraulic single cell flotation unit that is similar in concept to a mineral flotation cell,

but must be designed for minimal footprint, minimal weight, high single pass efficiency, gas and oil slugs, suspended solids, motion sensitivity, high uptime, and simplistic operation.

REFERENCES

Argaud, M.J. 1992. Predicting the interfacial tension of brine/gas (or condensates) system. *Advances in Core Evaluation III Reservoir Management, Reviewed Proceedings of the Society of Core Analysts Third European Core Analysis Symposium* in Paris, France. 14-16 September, 1992. 147-174.

Barkman, J.H. and Davidson, D. H. 1972. Measuring water quality and predicting well impairment. *Jour. Pet. Tech.* 24:865-873.

Bassett, M.G. 1971. WEMCO Depurator™ system. *SPE paper 3349 presented at the Rocky Mountain Regional Meeting of the Society of Petroleum Engineers of AIME* held in Billings, MT, 2-5 June 1971.

Department of Energy, Energy Information Administration (DOE/EIA). 2009. *March 2009 International Petroleum Monthly*, April 13, 2009. http://www.eia.doe.gov/ipm/supply.html

Ditria, J. C. and Hoyack, M. E. 1994. The separation of solids and liquid with hydrocyclone-based technology for water treatment and crude processing. *SPE paper 28815 presented at the SPE Asia Pacific Oil & Gas Conference* held in Melbourne, Australia, 7-10 November 1994.

Fuerstenau, M. C., Jameson, G., and Yoon, R.-H. 2007. *Froth Flotation-A Century of Innovation*. Society for Mining, Metallurgy, and Exploration, Inc., Littleton, CO. 357-358.

Grattoni, C., Moosai, R., and Dawe, R.A. 2003. Photographic observations showing spreading and non-spreading of oil on gas bubbles of relevance to gas flotation for oily wastewater cleanup. *Colloids and Surfaces A: Physiochem. Eng. Aspects* 214: 151-155.

Gutkowski, B., Hupka, J., and Miller, J.D. 1981. Flotation of oil droplets from water. In: *Interfacial Phenomena in Mineral Processing: Proceedings of the Engineering Foundation Conference*; Franklin Pierce College, Rindge, New Hampshire, August 2-7, 1981. 287-301.

Jennings, H.Y. and Newman, G.H. 1971. The effect of temperature and pressure on the interfacial tension of water against methane-normal decane mixtures. *Trans. AIME* 251:171-175.

McCain, W.D. 1990. *The Properties of Petroleum Fluids, 2nd edition*. Pennwell Publishing Company, Tulsa, OK, 1990.

Moosai, R., and Dawe, R.A. 2003. Gas attachment of oil droplets for gas flotation for oily wastewater cleanup. *Sep. Purif. Tech.* 33: 303-314.

Niewiadomski, M., Nguyen, A.V., Hupka, J., Nalaskowski, J., and Miller, J.D. 2007. Air bubble and oil droplet interactions in centrifugal fields during air-sparged hydrocyclone flotation. *Intl. J. of Environ. Pollution* 30.2: 313-331.

Oliveira, R.C.G., Gonzales, G., and Oliveira, J.F. 1999. Interfacial studies on dissolved gas flotation of oil droplets for water purification. *Colloids and Surfaces* 154: 127-135.

Rawlins, C.H. and Wang, I.I. 2000. Design and installation of a sand separation and handling system for a Gulf of Mexico oil production facility. *SPE paper 63041 presented at the 2000 SPE Annual Technical Conference and Exhibition* held in Dallas, TX, 1–4 October 2000.

Rawlins, C.H. 2009. Flotation cell design for produced water treatment: Phase 1 – analysis of intellectual property. Internal report. 20 January 2009.

Rawlins, C.H. 2009. Flotation of Fine Oil Droplets in Petroleum Production Circuits., *Mineral Processing Plant Design 2009*, Society for Mining, Metallurgy, and Exploration and The Minerals, Metals, and Materials Society, Tucson, AZ, Sep. 30 – Oct. 3, 2009.

Rodrigues, R.T. and Rubio, J. 2007. DAF-dissolved air flotation: potential applications in the mining and mineral processing industry. *Intl. J. Min. Proc.* 82: 1-13.

Sport, M.C. 1970. Design and operation of dissolved-gas flotation equipment for the treatment of oilfield produced brines. *SPE paper 2717 presented at the First Annual Offshore Technology Conference* held in Houston, TX, 18-21 May 1969.

Street, R.L., Watters, G.Z., and Vennard, J.K. 1996. *Elementary Fluid Mechanics, 7th edition*. John Wiley & Sons, Inc., 1996.

Strickland, W.T. 1979. Laboratory results of cleaning produced water by gas flotation. *SPE Paper 7805 Presented at the SPE 1979 Production Operators Symposium*, Oklahoma City, OK, 25-27 February, 1979.

Sylvester, N.D. and Byeseda, J.J. 1979. Oil/water separation by induced-air flotation. *SPE 7886 Presented at the SPE 1979 International Symposium on Oilfield and Geothermal Chemistry*, Houston, TX, 22-24 January, 1979.
Veil, J.A. 2009. The inextricable linkage of water and energy. *19th Produced Water Seminar*, January 14-16, 2009.